Journal of Orthopaedic Translation 47 (2024) 207–222

Contents lists available at ScienceDirect

Journal of Orthopaedic Translation

journal homepage: www.journals.elsevier.com/journal-of-orthopaedic-translation

Original article

TBK1 pharmacological inhibition mitigates osteoarthritis through attenuating inflammation and cellular senescence in chondrocytes

Rui Lu [b], Yunkun Qu [a], Zhenggang Wang [a], Zhiyi He [a], Shimeng Xu [a], Peng Cheng [a], Zhengtao Lv [a], Hongbo You [a], Fengjing Guo [a], Anmin Chen [a,**], Jiaming Zhang [c,***], Shuang Liang [a,*]

[a] Department of Orthopedics, Tongji Hospital, Tongji Medical College, Huazhong University of Science and Technology, Wuhan, 430030, China
[b] Department of Thoracic Surgery, Zhongnan Hospital of Wuhan University, Wuhan, 430030, China
[c] Clinical Innovation & Research Center (CIRC), Shenzhen Hospital, Southern Medical University, Shenzhen, 518100, China

ARTICLE INFO

Keywords:
BX795
Chondrocyte
Inflammation
Osteoarthritis
Senescence
TBK1

ABSTRACT

Objectives: TANK-binding kinase 1 (TBK1) is pivotal in autoimmune and inflammatory diseases, yet its role in osteoarthritis (OA) remains elusive. This study sought to elucidate the effect of the TBK1 inhibitor BX795 on OA and to delineate the underlying mechanism by which it mitigates OA.

Methods: Interleukin-1 Beta (IL-1β) was utilized to simulate inflammatory responses and extracellular matrix degradation *in vitro*. In vivo, OA was induced in 8-week-old mice through destabilization of the medial meniscus surgery. The impact of BX795 on OA was evaluated using histological analysis, X-ray, micro-CT, and the von Frey test. Additionally, Western blot, RT-qPCR, and immunofluorescence assays were conducted to investigate the underlying mechanisms of BX795.

Results: Phosphorylated TBK1 (P-TBK1) levels were found to be elevated in OA knee cartilage of both human and mice. Furthermore, intra-articular injection of BX795 ameliorated cartilage degeneration and alleviated OA-associated pain. BX795 also counteracted the suppression of anabolic processes and the augmentation of catabolic activity, inflammation, and senescence observed in the OA mice. In vitro studies revealed that BX795 reduced P-TBK1 levels and reversed the effects of anabolism inhibition, catabolism promotion, and senescence induction triggered by IL-1β. Mechanistically, BX795 inhibited the IL-1β-induced activation of the cGAS–STING and TLR3–TRIF signaling pathways in chondrocytes.

Conclusions: Pharmacological inhibition of TBK1 with BX795 protects articular cartilage by inhibiting the activation of the cGAS–STING and TLR3–TRIF signaling pathways. This action attenuates inflammatory responses and cellular senescence, positioning BX795 as a promising therapeutic candidate for OA treatment.

The translational potential of this article: This study furnishes experimental evidence and offers a potential mechanistic explanation supporting the efficacy of BX795 as a promising candidate for OA treatment.

1. Introduction

Osteoarthritis (OA), a prevalent age-related degenerative joint disease, manifests through articular cartilage destruction, osteophyte formation, subchondral bone remodeling, and recurrent synovitis [1]. This condition predominantly impacts knees, hips, interphalangeal, and intervertebral joints, leading to significant pain and dysfunction [2]. OA considerably reduces the quality of life for those affected and imposes a substantial economic burden, representing about 2.5 % of the Gross Domestic Product in developed countries [3]. The pathology of OA is characterized by chronic inflammation of chondrocytes, driven by various inflammatory mediators, leading to an imbalance between anabolism and catabolism within the articular cartilage [4]. Additionally, chondrocyte senescence, induced by external stimuli, oncogenic signaling, radiation, DNA damage, and oxidative stress, significantly contributes to OA pathogenesis by fostering chronic inflammation and

* Corresponding author.
** Corresponding author.
*** Corresponding author.
E-mail addresses: anminchenhust@126.com (A. Chen), jiaming_zhangtjmc@icloud.com (J. Zhang), liangshuang0310@tjh.tjmu.edu.cn (S. Liang).

https://doi.org/10.1016/j.jot.2024.06.001
Received 10 August 2023; Received in revised form 19 March 2024; Accepted 2 June 2024
2214-031X/© 2024 The Authors. Published by Elsevier B.V. on behalf of Chinese Speaking Orthopaedic Society. This is an open access article under the CC BY-NC-ND license (http://creativecommons.org/licenses/by-nc-nd/4.0/).

matrix degeneration through the secretion of senescence-associated secretory phenotype (SASP), comprising various inflammatory cytokines and growth factors [5]. However, the precise mechanisms underpinning these processes remain largely undefined. Identifying regulatory factors that modulate the chondrocyte inflammatory response and understanding their mechanisms have become crucial research objectives for OA treatment.

Our current understanding of OA pathology is evolving from viewing it as solely a mechanical wear-and-tear disease to recognizing it as a complex interplay of biomechanics, inflammation, and immune regulation [6]. It is now acknowledged that damage-associated molecular patterns (DAMPs) and pathogen-associated molecular patterns (PAMPs), which are pivotal in chronic inflammation and autoimmune disorders [7], play significant roles in OA. These endogenous signaling molecules are identified by pattern recognition receptors (PRRs) such as RIG-I-like receptors, cyclic GMP–AMP synthase (cGAS), the interleukin (IL)-1 receptor (IL-1R), and toll-like receptors (TLRs) [8]. cGAS acts as a cytosolic dsDNA sensor, initiating the stimulator of interferon genes (STING) signaling, which in turn activates transcription factors like IFN regulator factor 3 (IRF3) and NF-κB, leading to inflammation, immune responses, cellular senescence, and apoptosis [9–12]. The TLR signaling pathway consists of the MyD88-dependent pathway common to all TLRs and an MyD88-independent pathway specific to the TLR3 and TLR4 signaling pathways [13,14]. Toll-interleukin-1 receptor domain-containing adapter inducing interferon-beta (TRIF) promotes TLR3 and TLR4 signaling, which subsequently activates the transcription factors NF-κB and IRF3, resulting in the production of proinflammatory cytokines, dysregulation of innate immunity, senescence, and apoptosis [8,15]. Inhibiting STING and TRIF-mediated pathways has been shown to mitigate inflammation, senescence, and apoptosis, thereby reducing the progression of degenerative diseases [16,17].

Among the PRRs that initiate proinflammatory cytokine transcription, TANK-binding kinase 1 (TBK1) is a critical kinase and a central node within the signaling network. It integrates signals from both intracellular and extracellular environments, serving as an essential regulator of various biological processes, including inflammation, senescence, immune responses, apoptosis, and innate immunity [18]. Innate immune response has been demonstrated in triggering certain inflammatory diseases [19]. TBK1 emerges as a key regulator of neuroinflammation, playing a vital role in conditions such as amyotrophic lateral sclerosis, frontotemporal dementia, and normal tension glaucoma [20]. Despite recent studies implicating TBK1 in OA pathology, findings have been inconsistent [21,22]. BX795, a specific small molecule inhibitor of TBK1 phosphorylation, has been shown to suppress TBK1-mediated inflammation, autophagy, and apoptosis [23,24]. However, its impact on OA has not been elucidated. This study aims to explore the effects of TBK1 pharmacological inhibition with BX795 on OA.

2. Materials and methods

2.1. Reagents

BX795 (CAS Number: 702675-74-9) and DMXAA ([5,6-dimethylxanthone-4-acetic acid]; CAS Number: 117570-53-3), obtained from Med Chem Express (Shanghai, China), were dissolved in dimethylsulfoxide (DMSO) and stored in the dark for subsequent use. Poly(I:C) (CAS Number: 42424-50-0) was obtained from Tocris Bioscience (Bristol, UK). Recombinant mouse IL-1β was purchased from R&D Systems (Minneapolis, MN, USA). Primary rabbit antibodies for western blotting and cellular immunofluorescence assay against phosphorylated TBK1 (P-TBK1) (#5483) and TBK1 (#38066) were obtained from Cell Signaling Technology ([CST], Beverly, MA, USA). For immunohistochemical (IHC) analysis, primary rabbit antibodies against P-TBK1 (AF8190) and TBK1 (28397-1-AP) were obtained from Affinity Biosciences (Affinity Biosciences, OH, USA) and Proteintech Group (Wuhan, Hubei, China), respectively. Primary rabbit antibodies against Aggrecan (13880-1-AP), Collagen II (28459-1-AP), matrix metalloproteinase (MMP)-1 (10371-2-AP), MMP13 (18165-1-AP), TRIF (23288-1-AP), SIRT1 (13161-1-AP), and P53 (10442-1-AP) as well as mouse antibodies against GAPDH (60004-1-Ig) and MMP3 (66338-1-Ig) were purchased from Proteintech Group (Wuhan, Hubei, China). Primary rabbit antibodies against SOX9 (#82630), iNOS (#68186), COX-2 (#12282), $P21^{WAF1/CIP1}$ (#64016), cGAS (#31659), STING (#13647), P–P38 (#4511), P38 (#8690), P-JNK (#4668), JNK (#9252), P-ERK (#4370), anti-ERK (#4695), P-IKKα/β (#2697), IKKα (#61294), IKKβ (#8943), P–P65 (#3033), and P65 (#8242) were obtained from CST (Beverly, MA, USA). Primary rabbit antibody against $P16^{INK4a}$ (sc1661) was obtained from Santa Cruz Biotechnology (California, USA). Trypsin, type II collagenase, and primary rabbit antibody against A disintegrin and metalloprotease with thrombospondin type I motifs (ADAMTS)-5 ([ADAMTS5]; A02802-1) were acquired from Boster (Wuhan, Hubei, China). Anti-rabbit and anti-mouse secondary antibodies were acquired from SAB (Nanjing, Jiangsu, China). DMEM/F12 culture medium was purchased from Hyclone (Logan, UT, USA) and fetal bovine serum (FBS) was purchased from BioInd (Biological Industries, Israel). RIPA lysis buffer, protease inhibitors, and phosphatase inhibitors for total protein extraction were obtained from Boster (Wuhan, China).

2.2. Isolation and culture of mice chondrocytes

Primary chondrocytes were isolated from the knee cartilage of 5-day-old C57BL/6 male mice as follows: mice were disinfected by immersion in 75 % alcohol, knee cartilage was collected and cut into granules, followed by incubation with 0.25 % trypsin for 0.5 h at 37 °C in a 5 % CO_2 incubator. Next, after centrifugation and removal of trypsin, 0.2 % type II collagenase was added into the tube and the chondrocytes were re-incubated for 4–6 h at 37 °C in a hybridization oven. Following re-centrifugation and removal of type II collagenase, the chondrocytes were resuspended and cultured in DMEM/F12 medium containing 10 % FBS in a cell incubator with 5 % CO_2 at 37 °C. The first one or two passages of chondrocytes were used for subsequent experiments.

2.3. Cell viability assay

We analyzed the potential cytotoxicity of IL-1β/BX795/DMXAA/Poly(I:C) against chondrocytes using the Cell Counting Kit-8 (CCK-8) assay. In brief, cells were cultured in 96-well plates (10,000 cells/well), incubated at 37 °C under 5 % CO_2 for 24 h, and then treated with different concentrations of the abovementioned reagents after cell adhesion. Subsequently, cell viability was assessed in terms of the optical density value, which was measured at 450 nm using a microplate reader (Bio-Rad, Richmond, USA).

2.4. Protein extraction and western blotting analysis

After chondrocytes were treated with the different interventions, the cells were lysed for 15 min on ice with a cell lysate mix consisting of the RIPA lysis buffer, protease inhibitors, and phosphatase inhibitors in a 100:1:1 ratio. The cells were then collected and lysed using ultrasound. After centrifugation at 12,000 r/min for 0.5 h at 4 °C to obtain a higher-purity protein sample; the protein concentration of each sample was determined by measuring its optical density at 562 nm using a microplate reader. After adding an appropriate ratio of protein loading buffer into the protein samples and mixing them thoroughly, the samples were denatured at 95 °C for 10 min and then stored in −20 °C. Protein samples of equal concentration were separated via SDS–PAGE and then transferred to a polyvinylidene difluoride (PVDF) membrane (Millipore, USA). Nonspecific binding to the membrane was blocked by incubation for 1 h in 5 % skimmed milk at room temperature and then the membrane was incubated overnight with primary antibodies at 4 °C, followed by incubation with a corresponding species-specific, horseradish

peroxidase-conjugated secondary antibody for 1 h at room temperature. Finally, proteins on the PVDF membranes were visualized using the Western ECL Substrate Kit (Bio-Rad, Richmond, USA) and analyzed using the Image Lab Software (Bio-Rad Laboratories, Hercules, CA, USA).

2.5. RNA extraction and reverse transcription-polymerase chain reaction (RT-PCR) analysis

An RNA extraction kit (Omega Bio-tek, USA) was used to collect the total RNA samples from chondrocytes according to the manufacturer's instructions. Next, RNA was reverse transcribed using a complementary DNA (cDNA) synthesis kit (Yeasen, Shanghai, China), and the produced cDNA was stored in the refrigerator. RT-PCR was performed using SYBR Green (Yeasen, Shanghai, China) and corresponding primers were listed in Table S1. The comparative Ct ($2^{-\Delta\Delta Ct}$) method was used to determine the relative mRNA expression levels of different genes.

2.6. Cell senescence staining

A senescence β-galactosidase staining kit (C0602, Beyotime, Shanghai, China) was used to detect senescence-associated β-galactosidase (SA-β-Gal) protein; upregulation of the activity of this protein indicates cellular senescence [25]. Chondrocytes were subjected to different pretreatments and then subjected to SA-β-Gal staining according to the manufacturer's instructions. Light microscopy was used to visualize the stained cells; blue-colored cells were recognized as senescent (i.e. SA-β-Gal-positive) cells.

2.7. Immunofluorescence cell staining

Chondrocytes were seeded on a 24-well plate (10,000 cells/well) for 24 h and then subjected to different treatments. The cells were then fixed in paraformaldehyde for 15 min, washed three times with PBS (5 min each wash), and then permeabilized with 0.2 % Triton X-100 for 5 min. After three washes with PBS (5 min each wash) and blocking with 5 % bovine serum albumin for 30 min, the cells were incubated with primary antibodies overnight at 4 °C at the indicated dilution for the detection of P-TBK1 (#5483, 1:50, CST, Beverly, MA, USA), TBK1 (#38066, 1:200, CST, Beverly, MA, USA), Aggrecan (13880-1-AP, 1:200, Proteintech, Wuhan, Hubei, China), Collagen II (28459-1-AP, 1:800, Proteintech, Wuhan, Hubei, China), P–P65 (#3033, 1:800, CST, Beverly, MA, USA), and $P16^{INK4a}$ (sc1661, 1:100, Santa Cruz, California, USA). After washing three times with PBS (5 min each wash), the cells were incubated with corresponding species-specific fluorescent secondary antibody labeled with Cy3 or fluorescein isothiocyanate (Boster, Wuhan, Hubei, China) in the dark at 37 °C for 1 h. Subsequently, cell nuclei were counterstained with a reagent containing DAPI for 10 min. Finally, the cells were washed three times with PBS (5 min each wash) and observed using a fluorescence microscope (Evos Fl Auto, Life Technologies, USA).

2.8. Destabilized medial meniscus (DMM)-induced OA mice models

Thirty-six 8-week-old male mice (C57BL/6J) were housed in specific-pathogen-free conditions in the Animal Center of Tongji Hospital, Tongji Medical College, Huazhong University of Science and Technology and all experimental procedures were approved by the ethics committee (Ethics No: TJH-202107008). Changes in mouse body weight before surgery and at euthanization are presented in Table S2; no significant differences in body weight were observed between groups. To demonstrate the effect of BX795 on mice OA *in vivo*, we adopted the DMM method to establish an animal model of OA, as previously described [26]. Mice were randomly allocated to one of three groups in equal numbers: SHAM, SHAM + BX795, DMM, and DMM + BX795. After achieving satisfactory anesthesia effect via intraperitoneal injection of 1 % pentobarbital, a sham operation, which included only joint capsulotomy and suturing surgery, was performed in the SHAM and SHAM + BX795 group, whereas DMM surgery was performed for OA models in the DMM and DMM + BX795 groups. All surgical operations were performed on the right knee joint of the mice. One week after surgery, intra-articular injection of vehicle or other treatment was performed for 8 weeks, twice per week, in the affected knee joint of all groups. Mice in the SHAM and DMM groups received 10 μL of vehicle (30 % PEG300, 5 % DMSO, and ddH_2O); mice in the SHAM + BX795 group and DMM + BX795 group received 10 μL of BX795 (0.0473 mg/kg).

2.9. Pain behavioral testing

The mechanical abnormal pain test was quantified by measuring the hind paw withdrawal response by a set of Von Frey Aesthesiometer (North Coast Medical, USA). Briefly, the animals were placed in individual chambers on top of a wire grid platform and were allowed to habituate themselves to their environment for 30 min before the test. The plantar surface of the hind paw was stimulated with a von Frey hair that was placed perpendicularly until the hair flexed. The filament was then left in place for 3s and the withdrawal threshold was recorded. A positive response was defined as a rapid withdrawal of the hind paw when the stimulus was applied [27,28]. The test was performed blind, and each animal was tested at least three times. The identity of the animal, as well as the study group, was not known to the investigator.

2.10. Micro-computed tomography (Micro-CT) imaging evaluation

Mice were euthanized and the right knee joints were fixed in 4 % paraformaldehyde for 24 h before performing micro-CT. The parameters of the micro-CT scanning system (Micro-CT Scanco Medical, Bassersdorf, Switzerland) used to acquire images were set to 70 kV and 114 μA, with a resolution of 10 μm. Scans comprised of approximately 1000 slices spanning the femur, tibia, and knee joint. After scanning, X-ray and three-dimensional (3D) images of the knee joints and data on osteophyte volume, bone volume (BV), bone volume/tissue volume (BV/TV), trabecular separation (Tb.Sp), trabecular number (Tb.N), and trabecular thickness (Tb.Th) were obtained from the micro-CT scanning system after processing using a circular region of interest to constrain the tomographic images. In order to analyze subchondral bone changes, the epiphysis of the proximal tibia was chosen as the region of interest. The area of interest included the region between the articular cartilage and the growth plate. The outline of the epiphysis was carefully selected without any outgrowing osteophyte [29].

2.11. Histological staining and analysis

Knee joint specimens were fixed in 4 % paraformaldehyde, thoroughly decalcified, and embedded in paraffin. The embedded knee joint specimens were cut into 5 μm sections for histological staining, including hematoxylin–eosin (HE), toluidine blue, safranin O/fast green, and IHC staining. IHC analysis was performed using antibodies against P-TBK1 (AF8190, 1:50, Affinity Biosciences, OH, USA), TBK1 (28397-1-AP, 1:100, Proteintech, Wuhan, Hubei, China), Aggrecan (13880-1-AP, 1:200, Proteintech, Wuhan, Hubei, China), Collagen II (28459-1-AP, 1:800, Proteintech, Wuhan, Hubei, China), MMP13 (18165-1-AP, 1:100, Proteintech, Wuhan, Hubei, China), iNOS (#68186, 1:600, CST, Beverly, MA, USA), and $P16^{INK4a}$ (sc1661, 1:100, Santa Cruz, California, USA). The Osteoarthritis Research Society International (OARSI) scoring system was used to assess the severity of OA [30].

2.12. Statistical analysis

All experiments were repeated at least three times. Kolmogorov–Smirnov test was applied to measure the normal distribution of the

data which were presented as mean ± standard deviation (SD). One-way analysis of variance followed by Dunnett's post hoc test were used to analyze differences among multiple comparisons. The Chi-square test was employed for the comparison of enumeration data which were reported as rates or percentages. A p-value of <0.05 was considered statistically significant.

3. Results

3.1. Expression of P-TBK1 is upregulated in human and mouse OA knee articular cartilage

Considering the role of TBK1 in the inflammatory response, senescence, and apoptosis, we designed experiments to determine whether TBK1 or P-TBK1 is involved in the pathogenesis of OA. *In vivo*, human normal or OA knee cartilage specimens were obtained from Tongji Hospital, Tongji Medical College, Huazhong University of Science and Technology, and the process was approved by the institution's ethics committee (Ethics No: TJ-IRB20220478). The clinical characteristics of specimen donors could be found in Table S3. IHC analysis of knee articular cartilage revealed that the expression of P-TBK1 was significantly upregulated in the human OA group compared with the normal group (Fig. 1A and B). Meanwhile, high expression of P-TBK1 was also observed in the mice DMM group compared with the SHAM group (Fig. 1E and F). However, no significant difference in the expression level of TBK1 was observed between the human normal group and OA group (Fig. 1C and D) nor between the mice SHAM group and DMM group (Fig. 1G and H). Besides, intra-articular injection of BX795 significantly downregulated the expression of P-TBK1, without changing the expression of TBK1 in DMM + BX795 group compared with the DMM group.

In vitro, we found that IL-1β, as an important cytokine that stimulates the inflammatory environment, could affect the expression of P-TBK1. The data revealed that the expression level of P-TBK1 in chondrocytes changed with the stimulation of IL-1β at different concentrations (0, 1, 2, 5, and 10 ng/mL IL-1β for 24 h) and durations (5 ng/mL IL-1β for 0, 1, 6, 12, 24, and 48 h). In detail, the expression of P-TBK1 was upregulated after treatment with IL-1β, the degree of elevation being positively correlated with the concentration of IL-1β, and increased to a relatively high level at 5 ng/mL and 10 ng/mL IL-1β for 24 h (Fig. 1I and J). Regarding the effect of IL-1β on the expression of P-TBK1 in chondrocytes at different time durations, the expression of P-TBK1 peaked at 1 h and then gradually decreased (Fig. 1I and J). However, the expression level of TBK1 in chondrocytes was sustained at a constant level, irrespective of the cells undergoing stimulation with IL-1β at different concentrations and durations. In addition, the change in the abovementioned western blot data about P-TBK1 expression was also verified via immunofluorescence analysis (Fig. 1K–N).

3.2. Viability of chondrocytes treated with IL-1β/BX795/DMXAA/poly (I:C)

The viability of chondrocytes treated with IL-1β/BX795/DMXAA/poly(I:C) was evaluated via CCK-8 assay. No evident cytotoxicity was observed when chondrocytes were stimulated with IL-1β at various concentrations (0, 1, 2, 5, and 10 ng/mL) for 24 h (Fig. S1A). Meanwhile, cells treated with 5 ng/mL IL-1β for different durations (0, 1, 6, 12, 24, and 48 h) did not exhibit significant growth inhibition (Fig. S1B). As for BX795, the data showed that although it was toxic to cells when the concentration reached 40 μM (Fig. S1C), concentrations below 40 μM had no remarkable effect on the viability of chondrocytes. We also observed the viability of chondrocytes treated with 5, 10, and 20 μM of BX795 with or without 5 ng/mL IL-1β for 24 h and found that there was no significant cytotoxicity to chondrocytes (Fig. S1D). Moreover, the viability of chondrocytes was not significantly affected when they were treated with 25 μM DMXAA or 10 μg/mL Poly(I:C) along with or without 20 μM BX795 (Figs. S1E and F).

3.3. The selection of proper concentration and time duration of IL-1β for establishing ideal OA chondrocytes

IL-1β is employed as a cytokine to establish an OA chondrocytes *in vitro*. We explored the appropriate concentration and time duration of IL-1β for establishing ideal OA chondrocytes. As shown in Figs. S2A and B, western bolt showed that the expression of anabolic proteins (Aggrecan, Collagen II, and SOX9) gradually decreased while catabolic proteins (MMP3 and MMP13) and inflammatory proteins (iNOS and COX-2) gradually increased with increasing concentration of IL-1β and reached a relatively ideal level at IL-1β concentrations of 5 and 10 ng/mL. Besides, with the prolongation of IL-1β stimulation, the expression of anabolic proteins (Aggrecan, Collagen II, and SOX9) gradually decreased while the catabolic proteins (MMP3 and MMP13) and inflammatory proteins (iNOS and COX-2) gradually increased with the prolongation of IL-1β stimulation and reached a relatively high level at 24 and 48 h (Figs. S2C and D). Considering the overall beneficial effect of IL-1β on chondrocytes for inhibiting anabolism and promoting catabolism and inflammatory responses, we selected an IL-1β concentration of 5 ng/mL to stimulate chondrocytes for 24 h for evaluating changes in their phenotypes of the following experiments.

3.4. BX795 reverses the inhibition of anabolism and enhancement of catabolism and inflammatory responses in IL-1β-induced chondrocytes

Cultured chondrocytes were stimulated with BX795 (5, 10 and 20 μM) and IL-1β (5 ng/ml) for 24 h. As shown in Fig. 2A and B, the expression of P-TBK1 increased and that of TBK1 was maintained at a constant level after IL-1β stimulation compared with the control group. However, compared with the IL-1β group, the expression of P-TBK1 decreased significantly ($p < 0.05$) after the administration of BX795 in IL-1β-induced chondrocytes. Anabolism and catabolism play a vital role in the homeostasis of the cartilage extracellular matrix (ECM). To further explore the effects of BX795, we investigated the promising effects of BX795 in anabolism and catabolism. The data demonstrated that IL-1β could inhibit anabolism in chondrocytes, whereas BX795 could reverse this effect. In brief, IL-1β downregulated the expression of anabolic proteins (Aggrecan, Collagen II, and SOX9), whereas various concentrations of BX795 (5, 10, and 20 μM) upregulated the expression of those proteins in a concentration-dependent manner (Fig. 2C and D). In addition, BX795 could suppress the enhancement of catabolism and inflammatory responses in IL-1β-treated chondrocytes. High expression of catabolic proteins (ADAMTS5, MMP1, MMP3, and MMP13) and inflammatory proteins (iNOS and COX-2) was observed in IL-1β-induced chondrocytes; however, BX795 downregulated the expression of these proteins and reversed the trend in a concentration-dependent manner (Fig. 2E, F, H, I). Furthermore, we verified the abovementioned western blot data using RT-PCR. The decrease in the mRNA expression of anabolic genes (Aggrecan, Collagen II, and SOX9) and increase in the mRNA expression of catabolic genes (ADAMTS5 and MMP13) in IL-1β-induced chondrocytes were reversed by BX795 (Fig. 2G). In addition, immunofluorescence analysis revealed that BX795 increased the downregulated expression of Aggrecan and Collagen II in IL-1β-induced chondrocytes (Fig. 2J-M). These findings indicate that BX795 maintained the metabolic homeostasis of the ECM and prevented ECM degradation by enhancing anabolism and inhibiting catabolism and the inflammatory response in chondrocytes.

3.5. BX795 inhibits IL-1β-induced senescence of chondrocytes

The effects of different concentrations and time durations of IL-1β on the senescence metabolism of chondrocytes is unknown, so we explored it in our study. The effects of different concentrations of IL-1β (0, 1, 2, 5, and 10 ng/mL IL-1β for 24 h) and different stimulation times (5 ng/mL

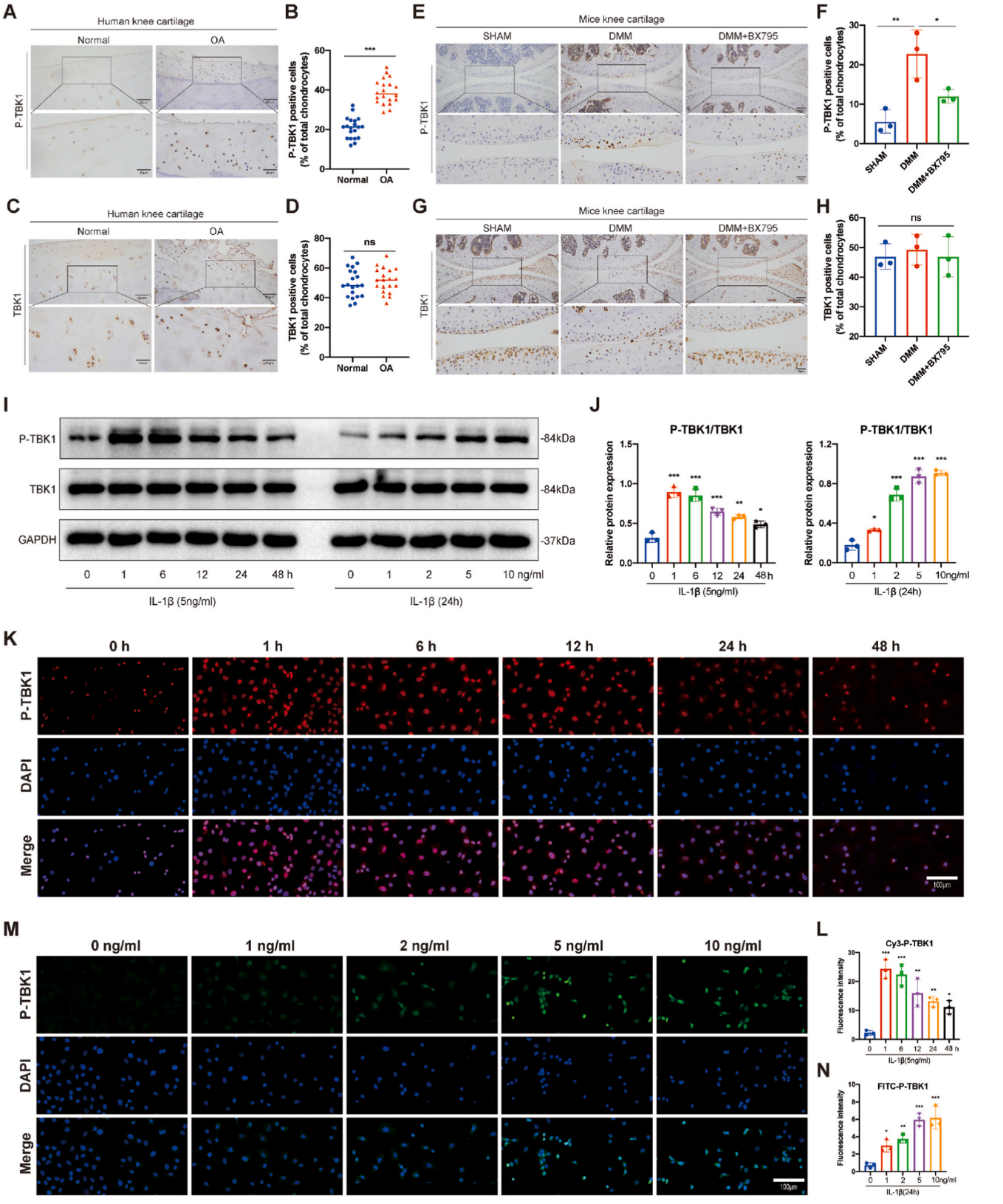

Figure 1. Expression levels of P-TBK1 and TBK1 in human and mouse knee articular cartilage. Immunohistochemical and quantitative analysis of positive chondrocytes were performed to determine the expression of P-TBK1 and TBK1 in human knee cartilage (A–D, n = 20) and mice knee cartilage (E–H, n = 3). (I, J) Expression levels of P-TBK1 in chondrocytes following stimulation with IL-1β at different concentrations (0, 1, 2, 5, and 10 ng/mL IL-1β for 24 h) and durations (5 ng/mL IL-1β for 0, 1, 6, 12, 24, and 48 h) (n = 3) as determined using western blot analysis. (K–N) Expression levels of P-TBK1 in chondrocytes following stimulation with IL-1β at different concentrations (0, 1, 2, 5, and 10 ng/mL IL-1β for 24 h) and durations (5 ng/mL IL-1β for 0, 1, 6, 12, 24, and 48 h) as determined using immunofluorescence staining (n = 3). Data are presented as means ± SD. *$p < 0.05$, **$p < 0.01$, ***$p < 0.001$. ns, no significance.

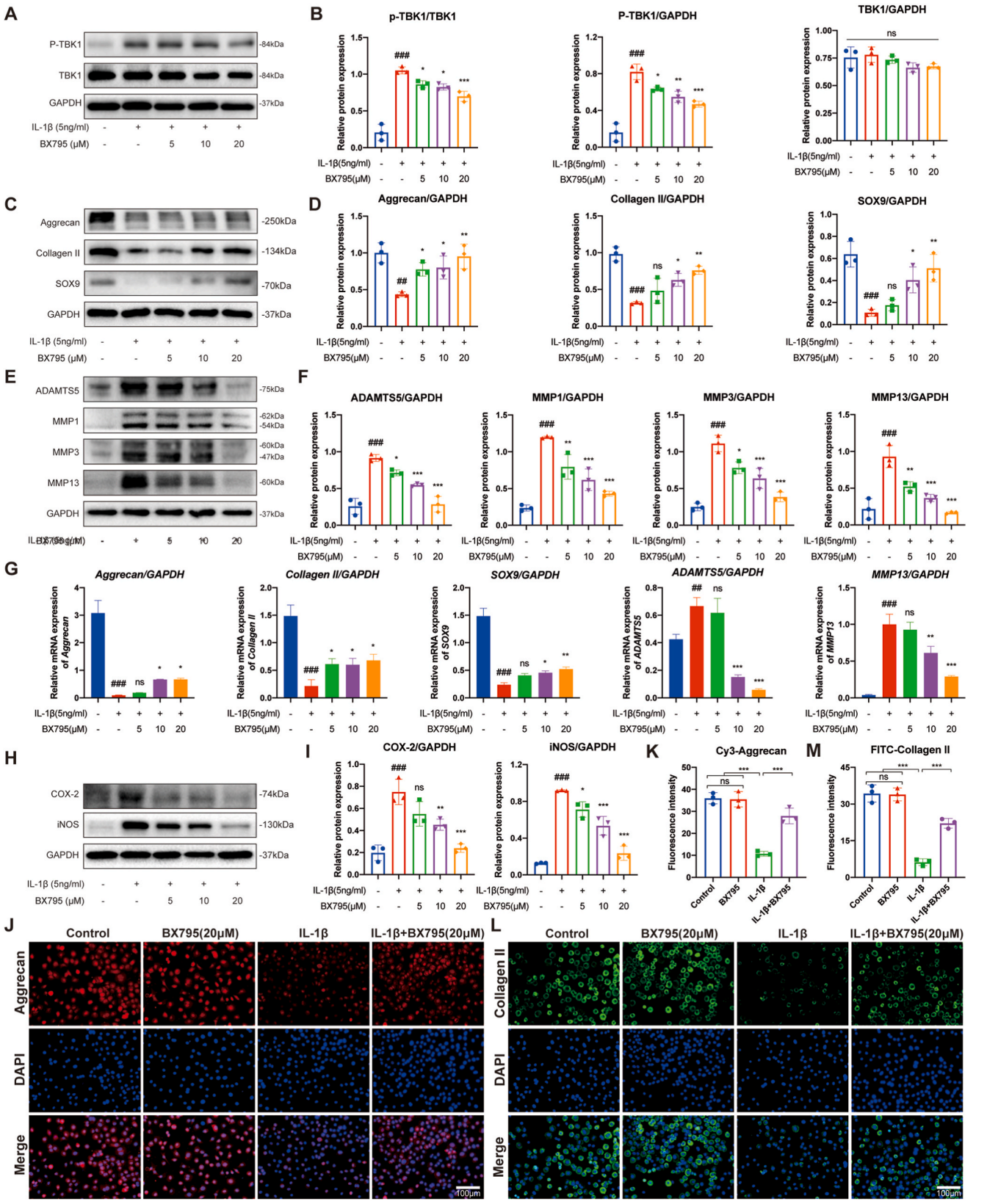

Figure 2. Effects of BX795 on IL-1β-induced chondrocyte anabolism, catabolism, and inflammatory response. (A) Western blot and (B) quantitative analyses of proteins (P-TBK1 and TBK1) in chondrocytes treated with IL-1β along with or without 5, 10, or 20 μM BX795. Expression of anabolic proteins (C, D), catabolic proteins (E, F), and inflammatory proteins (H, I) was evaluated using western blot and quantitative analysis. (G) RT-PCR was performed to determine the expression levels of Aggrecan, Collagen II, SOX9, ADAMTS5, and MMP13. Immunofluorescence staining of Aggrecan (J, K) and Collagen II (L, M) and quantitative analysis of their expression levels. Data are presented as means ± SD (n = 3). ##$p < 0.01$; ###$p < 0.001$ compared with control group. ns, no significance; *$p < 0.05$; **$p < 0.01$; ***$p < 0.001$ compared with IL-1β group.

IL-1β for 0, 1, 6, 12, 24, and 48 h) on chondrocyte senescence phenotypes were measured using western blot analysis. As shown in Fig. 3A and B, the negative senescence-associated phenotypic protein (SIRT1) gradually decreased while the positive senescence-associated phenotypic proteins (P53, $P21^{WAF1/CIP1}$, and $P16^{INK4a}$) gradually increased with increasing concentration of IL-1β and reached a relatively ideal level at IL-1β concentrations of 5 and 10 ng/mL. Besides, the protein SIRT1 gradually decreased while P53, $P21^{WAF1/CIP1}$, and $P16^{INK4a}$ gradually increased with the prolongation of IL-1β stimulation and reached a relatively ideal level at 24 and 48 h (Fig. 3C and D). Thus, considering the overall beneficial effect of IL-1β on chondrocytes senescence-associated phenotypes, 5 ng/mL IL-1β to stimulate chondrocytes for 24 h for establishing an ideal cell senescence model.

Afterwards, to determine the effects of BX795 on IL-1β induced senescence of chondrocytes, the expression of senescence-associated secretory phenotype (SASP) factors, including SITR1, P53, $P21^{WAF1/CIP1}$, and $P16^{INK4a}$ were measured. As shown in Fig. 3A and B, IL-1β promoted the senescence of chondrocytes, as the expression of the SITR1 decreased and that of P53, $P21^{WAF1/CIP1}$, and $P16^{INK4a}$ increased compared with the control group. However, treatment with BX795 inhibited the IL-1β-induced senescence of chondrocytes, as BX795 upregulated the expression of SIRT1 and downregulated that of P53, $P21^{WAF1/CIP1}$, and $P16^{INK4a}$ (Fig. 3E and F). In addition, SA-β-Gal staining for senescence revealed that the number of SA-β-gal-positive chondrocytes increased after stimulation with IL-1β and decreased after BX795 treatment (Fig. 3G and H).

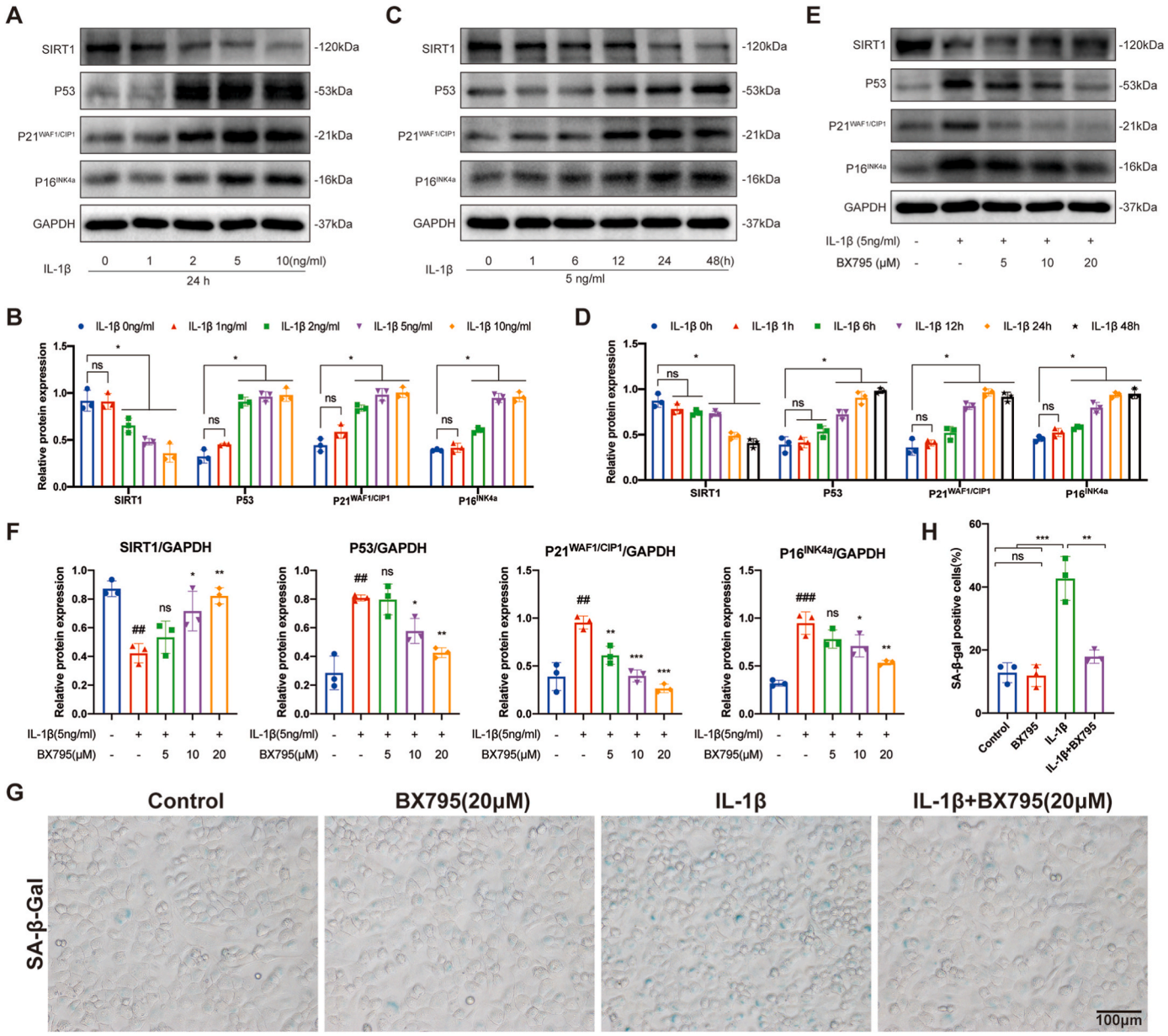

Figure 3. Effects of BX795 on IL-1β-induced chondrocyte senescence (A, C) Western blot data and (B, D) quantitative analysis of the expression levels of senescence-associated phenotypic proteins (SIRT1, P53, $P21^{WAF1/CIP1}$, and $P16^{INK4a}$) in chondrocytes treated with different concentrations of IL-1β (0, 1, 2, 5, and 10 ng/mL IL-1β for 24 h) and different stimulation times (5 ng/mL IL-1β for 0, 1, 6, 12, 24, and 48 h). (E) Western blot data and (F) quantitative analysis of the expression levels of senescence-associated phenotypic proteins (SIRT1, P53, $P21^{WAF1/CIP1}$, and $P16^{INK4a}$) in chondrocytes treated with 5 ng/mL IL-1β along with or without 5, 10, and 20 μM BX795 for 24 h. (G) SA-β-Gal staining and (H) quantitative analysis of senescence-positive chondrocytes (SA-β-Gal-positive cells) in chondrocytes treated with IL-1β along with or without 20 μM BX795. Data are presented as means ± SD (n = 3). $##p < 0.01$; $###p < 0.001$ compared with control group. ns, no significance; $*p < 0.05$; $**p < 0.01$; $***p < 0.001$ compared with IL-1β group.

3.6. BX795 inhibits DMXAA-induced chondrocyte inflammation and senescence via the cGAS–STING–TBK1 signaling pathway

Recent study indicated that cGAS/STING signaling pathway modulate the expression of proinflammatory genes in OA cartilage [31]. To analyze whether the TBK1 mediated expression of proinflammatory genes is dependent on cGAS/STING pathway, we analyzed the production of cGAS and STING in the inactivation of TBK1. The protein

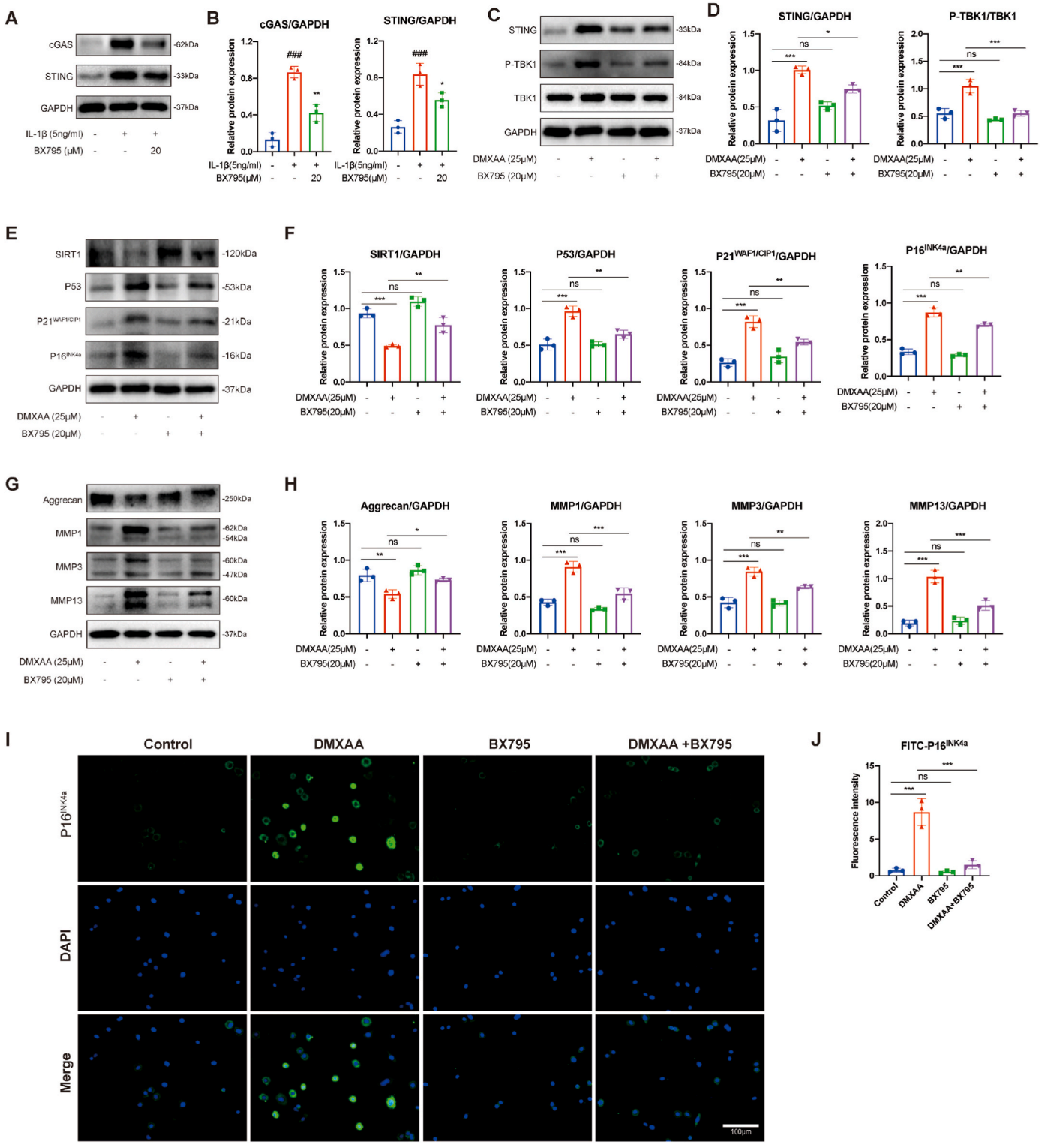

Figure 4. Protection of BX795 against DMXAA-induced cGAS–STING–TBK1 signaling pathway-dependent chondrocyte senescence, anabolism, and catabolism. (A, B) Protein expression levels of cGAS and STING evaluated by western blot analysis. (C, D) Expression of proteins (STING, P-TBK1, and TBK1) in the cGAS–STING–TBK1 signaling pathway was evaluated using western blot analysis. Expression of senescence-associated phenotypic proteins (E, F) and anabolic and catabolic proteins (G, H) in chondrocytes were determined using western blot analysis. (I, J) Immunofluorescence staining and quantitative analysis of the expression levels of $P16^{INK4a}$. Data are presented as means ± SD (n = 3). ns, no significance, $*p < 0.05$; $**p < 0.01$; $***p < 0.001$.

expression of cGAS and STING increased following IL-1β stimulation of chondrocytes; however, the administration of BX795 decreased the expression of these proteins (Fig. 4A and B). Next, DMXAA was used to activate STING and our results proved that the expression of STING increased following the administration of 25 μM DMXAA. However, BX795 attenuated this activation (Fig. 4C and D). In addition, similar to the stimulating effect of IL-1β, DMXAA increased the P-TBK1/TBK1 ratio compared with the control group, whereas BX795 decreased this ratio in DMXAA-induced chondrocytes (Fig. 4C and D). DMXAA also promoted cellular senescence, upregulated the expression of catabolic proteins (MMP1, MMP3, and MMP13), and downregulated the expression of the anabolic protein Aggrecan, whereas BX795 reversed all these effects (Fig. 5E–H). The abovementioned western blot data about $P16^{INK4a}$ was also verified via immunofluorescence analysis (Fig. 5I and J). These results indicate that the TBK1 inhibitor BX795 suppresses the occurrence of chondrocyte senescence, enhancement of catabolism, and attenuation of anabolism via the cGAS–STING–TBK1 signaling pathway.

3.7. BX795 inhibits Poly(I:C)-induced chondrocyte inflammation and senescence via the TLR3–TRIF–TBK1 signaling pathway

Recognition of TLRs by IL-1β stabilizes recruitment of one essential adaptor protein, TRIF, to induce inflammatory response in OA [32]. To analyze whether the TBK1 mediated expression of proinflammatory genes is dependent on TLR3–TRIF pathway, we also analyzed the expression of TRIF in the inactivation of TBK1. The administration of BX795 decreased the expression of TRIF induced by IL-1β (Fig. 5A and B). Poly(I:C), an agonist of TLR3 that exclusively engages TRIF, was used to assess the function of TRIF in inflammatory response. Our results confirmed that Poly(I:C) upregulated the expression of TRIF; however, BX795 attenuated this effect (Fig. 5C and D). Meanwhile, similar to the activity of DMXAA, Poly(I:C) elevated the ratio of P-TBK1/TBK1 compared with the control group, whereas BX795 decreased this ratio compared with the Poly(I:C)-induced chondrocytes (Fig. 5C and D). In addition, Poly(I:C) promoted cellular senescence, increased the production of catabolic proteins (MMP1, MMP3, and MMP13), and decreased the expression of the anabolic protein aggrecan. However, the expression of these proteins was reversed following the administration of BX795 in Poly(I:C)-induced chondrocytes (Fig. 5E–H). The abovementioned western blot data about $P16^{INK4a}$ was also verified via immunofluorescence analysis (Fig. 5I and J). These results suggest that the TBK1 inhibitor BX795 suppresses the occurrence of chondrocyte senescence, enhancement of catabolism, and attenuation of anabolism via TLR3–TRIF–TBK1 signaling pathway.

3.8. BX795 inhibits IL-1β-induced activation of the MAPK and NF-κB signaling pathways

Previous studies have revealed that MAPK and NF-κB signaling pathways are two crucial downstream signal transduction nodes that regulate inflammatory responses, ECM homeostasis, and OA progression [33,34]. Therefore, these two signaling pathways has been studied. The results (Fig. 6A–D) confirmed the early activation of these pathways, as the phosphorylation of JNK, ERK, P38, IKKα/β, and P65 (P-JNK, P-ERK, P–P38, P-IKKα/β, and P–P65) increased compared with the control group, whereas JNK, ERK, P38, IKKα, IKKβ, and P65 protein levels were relatively constant in all groups. Moreover, the expression of P-JNK, P-ERK, P–P38, and P–P65 peaked following 15 min of IL-1β stimulation and decreased gradually with increasing IL-1β exposure time (30, 60, and 120 min). Based on these results, the two pathways were maximally activated when chondrocytes were stimulated with IL-1β for 15 min, which was the time applied for subsequent studies of BX795.

With respect to the MAPK signaling pathway, the expression of P-JNK, P-ERK, and P–P38 was significantly increased after chondrocytes were treated with IL-1β for 15 min compared with the control group. However, P-JNK and P–P38 but not P-ERK levels decreased after the administration of BX795 (Fig. 6E and F). Regarding NF-κB signaling, compared with the control group, IL-1β triggered the phosphorylation of IKKα/β, IKBα, and P65 (P-IKKα/β, P-IKBα, and P–P65) and decreased the protein expression of IKBα, but no remarkable effect was observed on the expression of IKKα, IKKβ, and P65. In addition, the increased protein expression of P-IKKα/β, P-IKBα, and P–P65 could be reversed by treating IL-1β-induced chondrocytes with BX795 (Fig. 6G and H). Moreover, cellular immunofluorescence analysis of P–P65 revealed its increased accumulation in the nucleus of IL-1β-induced chondrocytes. However, BX795 reduced the tendency of P–P65 to accumulate in the nucleus (Fig. 6I and J). These findings suggest that BX795 partially inhibits the activation of the MAPK and NF-κB signaling pathways in IL-1β-induced chondrocytes.

3.9. BX795 attenuates the progression of OA in DMM mice

To investigate the effects of BX795 on OA *in vivo*, we established the DMM mice model, followed by intra-articular injection of BX795 twice per week for eight weeks. From a macroscopic point of view (Fig. 7A and B), using X-ray and micro-CT analyses, the knee joint surface of the mice in the SHAM and SHAM + BX795 group was smooth and without cartilage destruction, osteophyte formation, joint space narrowing, or other cartilage degeneration changes, whereas mice in the DMM group exhibited obvious OA changes, such as cartilage roughening, osteophyte formation, and joint space narrowing. However, the abovementioned OA changes were alleviated to a certain extent in the DMM + BX795 group. Compared with DMM group, the volume of osteophyte were prominently reduced in BX795 treated DMM mice (Fig. 7D, E). Furthermore, bone remodeling of the subchondral bone in the tibial plateau was observed. As shown in Fig. 7D, E, BV, BV/TV, Tb.N, and Tb.Th in the tibial plateau were lower in the DMM group than that in the SHAM and SHAM + BX795 group, whereas Tb.Sp in the tibial plateau was higher in the DMM group than that in the SHAM and SHAM + BX795 group. As the above parameters reflecting bone remodeling of the subchondral bone in the tibial plateau were reversed in the DMM + BX795 group, BX795 therefore inhibited bone destruction. In pain-related behavioral tests, a series of behavioral tests were performed to determine whether mechanical allodynia increased in the mice after intra-articular injection of BX795. The von Frey test results showed that there was a tremendous alteration of nociceptive reaction in DMM mice compared to those in the SHAM and SHAM + BX795 group from the second week after operation. However, this exacerbated DMM-mediated pain was partly ameliorated after BX795 treatment, suggesting that OA-associated pain was alleviated by BX795 treatment (Fig. 7C).

From a microscopic point of view, HE, toluidine blue, and safranin O/fast green staining revealed gross morphological changes in the cartilage (Fig. 8A), in which the curvature of normal articular cartilage surface in the SHAM and SHAM + BX795 group was smooth and without any roughness, whereas significant superficial articular cartilage erosion and reduced cartilage thickness were observed in the DMM group. Further, proteoglycan loss was observed in the DMM group compared with the SHAM and SHAM + BX795 group. However, the adverse effects of articular cartilage destruction were alleviated by BX795 treatment, as evidenced by less cartilage erosion and more proteoglycans present in the DMM + BX795 group compared with those in the DMM group. The OARSI score, which reflects the degree of OA, confirmed that BX795 alleviated the progression of OA (Fig. 8B).

In addition, IHC staining was performed to assess the amount of various key proteins associated with anabolism, catabolism, inflammation, and senescence in OA chondrocytes *in vivo*. For anabolism, catabolism, inflammation, and senescence indicator, decreased amounts of Aggrecan and Collagen II, increased amounts of MMP13, iNOS, and $P16^{INK4a}$ were observed in the DMM group compared with the SHAM and SHAM + BX795 group. In contrast, we observed the increased expression of Aggrecan and Collagen II and decreased expression of MMP13, iNOS, and $P16^{INK4a}$ in the DMM + BX795 group (Fig. 8C and

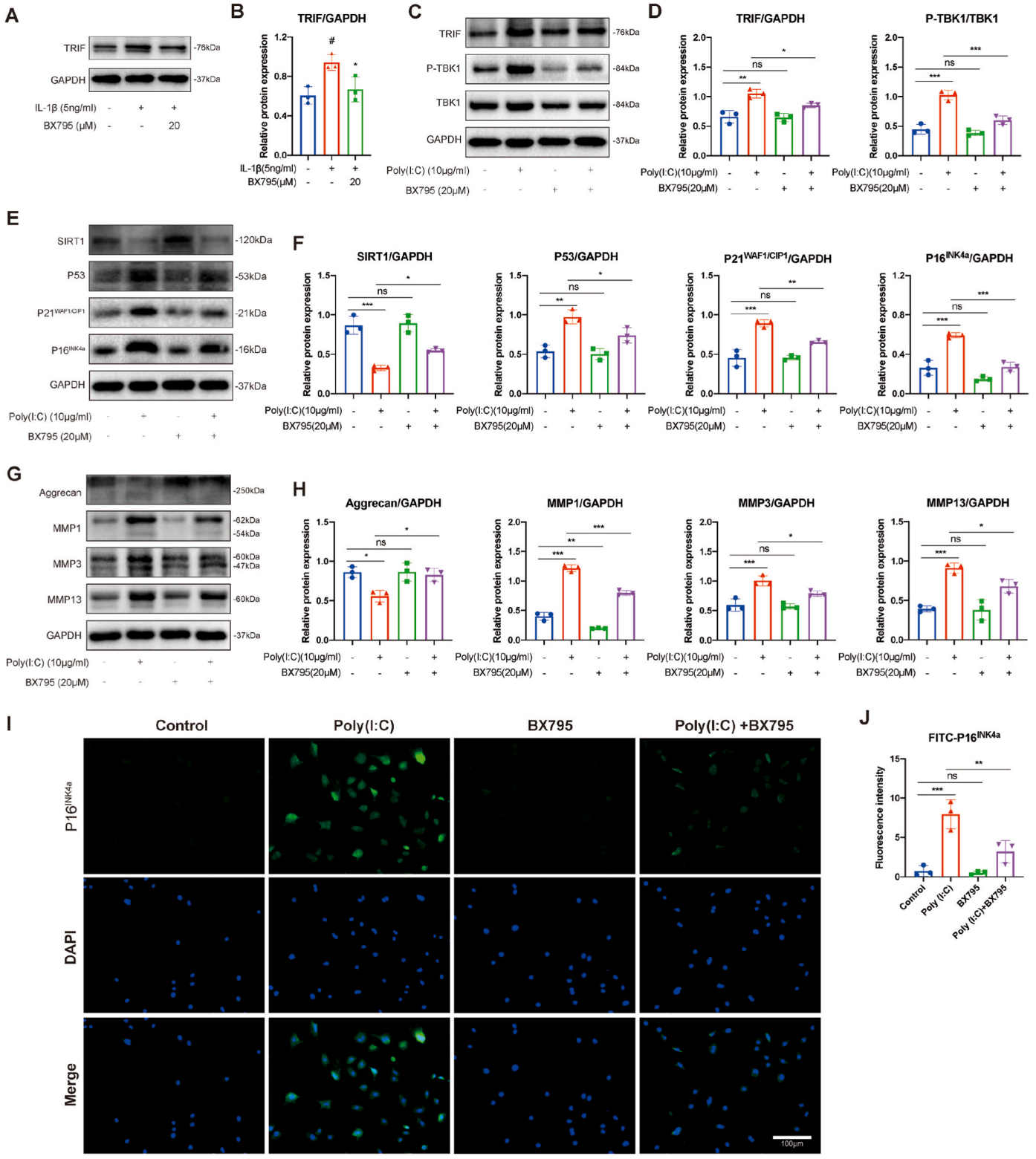

Figure 5. Protection of BX795 against Poly(I:C)-induced TLR3–TRIF–TBK1 signaling pathway-dependent chondrocyte senescence, anabolism, and catabolism. (A, B) Protein expression levels of TRIF evaluated by western blot analysis. (C, D) Expression of proteins (TRIF, P-TBK1, and TBK1) in the TLR3–TRIF–TBK1 signaling pathway was evaluated using western blot analysis. Expression of chondrocyte senescence-associated phenotypic proteins (E, F) and anabolic and catabolic proteins (G, H) were determined using western blot analysis. (I, J) Immunofluorescence staining and quantitative analysis of the expression levels of $P16^{INK4a}$. Data are presented as means ± SD (n = 3). ns, no significance, $*p < 0.05$; $**p < 0.01$; $***p < 0.001$.

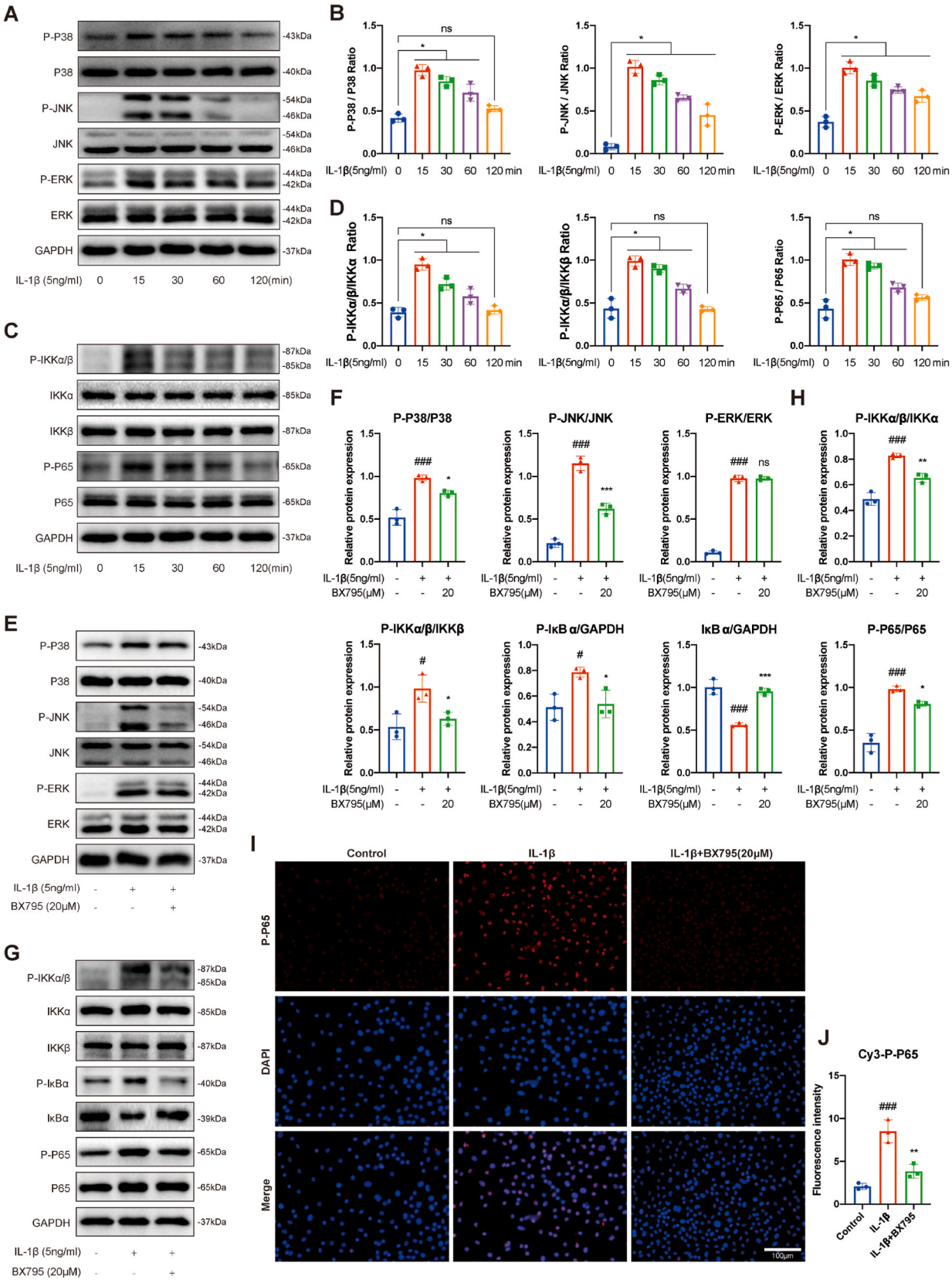

Figure 6. Effects of BX795 on MAPK and NF-κB signaling pathways. Western blot and quantitative analysis showed the activation of MAPK (A, B) and NF-κB (C, D) signaling pathways in chondrocytes treated with 5 ng/mL IL-1β at different time points (0, 15, 30, 60, and 120 min). Western blot and quantitative analyses showed that BX795 affected MAPK (E, F) and NF-κB(G, H) signal-related proteins. (I) Immunofluorescence staining and (J) quantitative analysis reflected the nuclear accumulation of P–P65 in chondrocytes treated with IL-1β alone or together with 20 μM BX795. Data are presented as means ± SD (n = 3). #$p < 0.05$; ###$p < 0.001$ compared with control group. ns, no significance, *$p < 0.05$; **$p < 0.01$; ***$p < 0.001$ compared with IL-1β group.

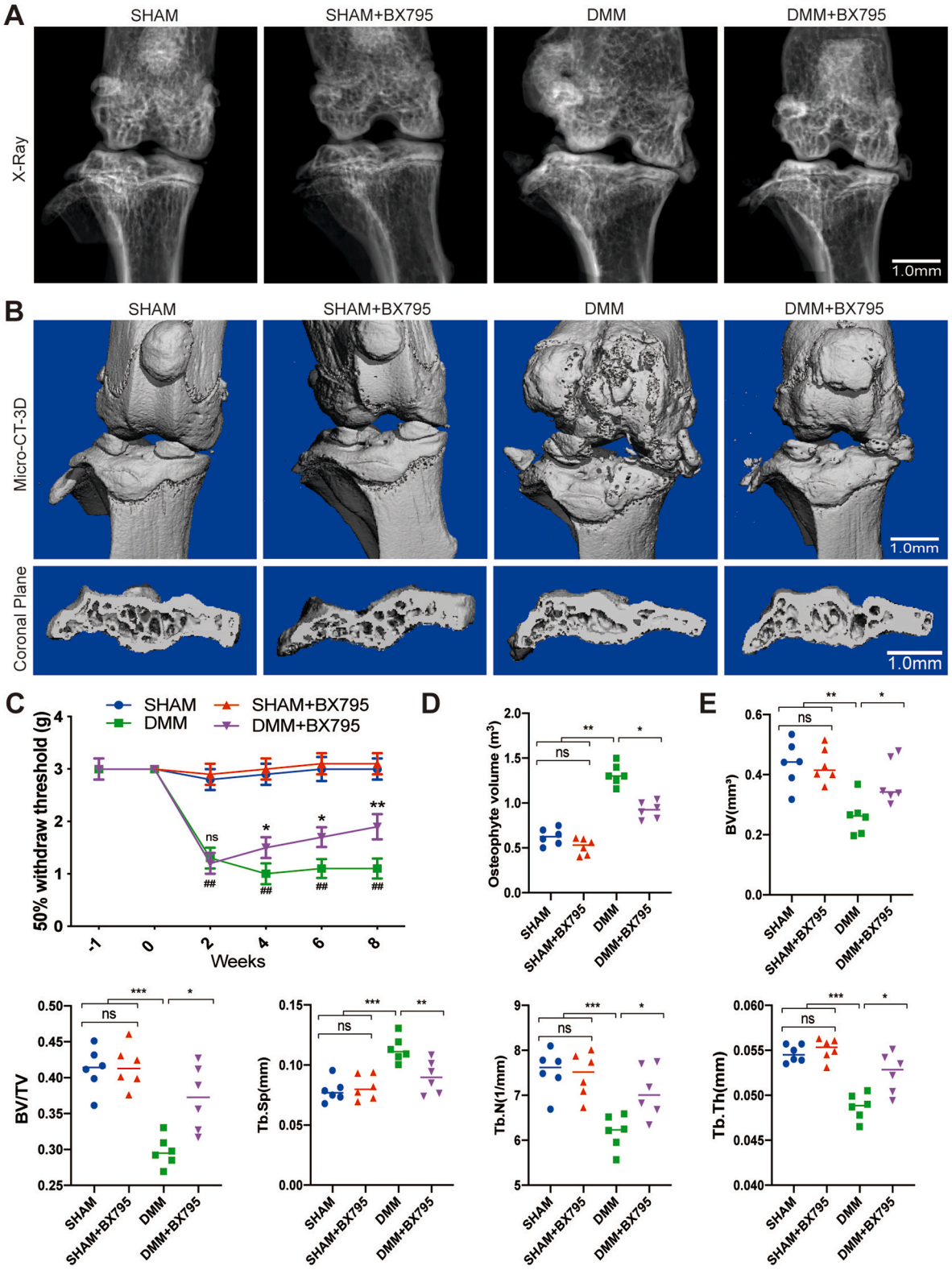

Figure 7. BX795 attenuated the progression of OA in DMM mice. (A, B) Images of X-Ray, Micro-CT-3D, and Coronal Plane about the knee joints exhibited a general view of knee cartilage changes in the SHAM, SHAM + BX795, DMM, DMM + BX795 groups. (C) Pain behavioral test assessed by von Frey test. Paw withdrawal threshold in response to von Frey filament stimulation at several time points. Results are presented as mean ± SD of 6 mice per group. # represents differences in values between the DMM and SHAM groups; * represents differences in values between the DMM and DMM + BX795 groups; (D, E) Quantitative analysis of subchondral bone remodeling parameters (osteophyte volume, BV, BV/TV, Tb.Sp, Tb.N, and Tb.Th) of tibial plateau in knee joints among the SHAM, SHAM + BX795, DMM, DMM + BX795 groups (n = 6). *p < 0.05; **p < 0.01; ***p < 0.001; ##p < 0.01.

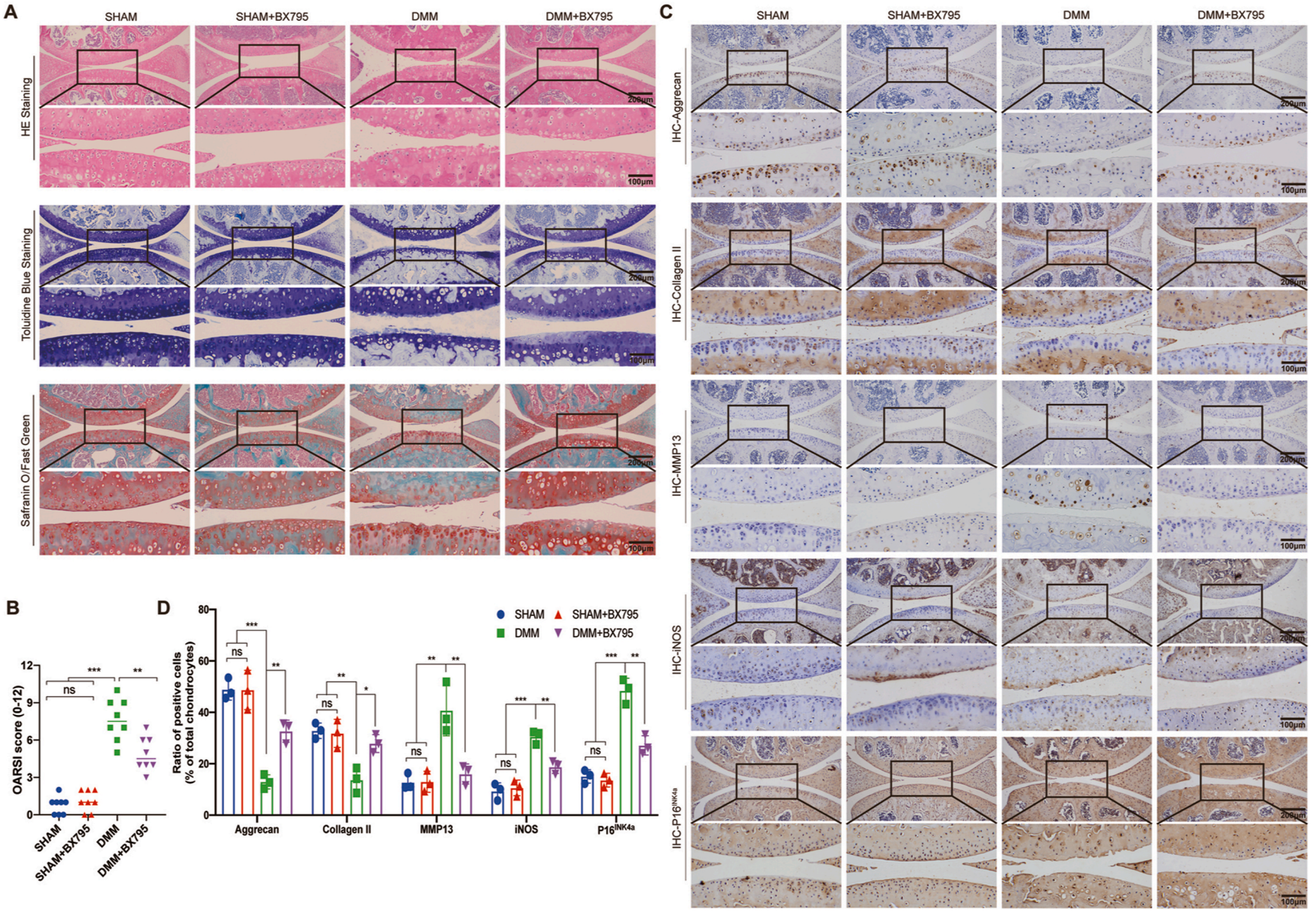

Figure 8. BX795 alleviated cartilage degradation and chondrocyte senescence in DMM mice. (A) HE, toluidine blue, and safranin O/fast green staining reflect the articular cartilage surfaces. (B) Quantitative analysis of the OARSI scores (n = 8). (C) Immunohistological staining and (D) quantitative analysis of anabolic (Aggrecan, Collagen II), catabolic (MMP13), inflammation (iNOS), and senescence-related ($P16^{INK4a}$) phenotypic proteins (n = 3). *p < 0.05; **p < 0.01; ***p < 0.001.

D), which indicates that BX795 exhibits articular cartilage protection properties. The above data suggest that intra-articular injection of BX795 may attenuate cartilage destruction in mice OA *in vivo*.

4. Discussion

Currently, treatment for OA primarily focuses on alleviating pain and enhancing joint function, underscoring the pressing need for more effective therapeutic options. This gap in treatment efficacy accentuates the critical demand for a disease-modifying osteoarthritis drug, which holds the potential to inhibit or even reverse the progression of OA. Accumulating studies have uncovered that TBK1 is involved in OA pathology [21,22]. Therefore, targeting TBK1 presents a promising approach for the treatment of OA. In this study, phosphorylated TBK1, rather than total TBK1, was significantly overexpressed in both animal and cell models of OA. Further analysis demonstrated that the TBK1 inhibitor, BX795, protects articular cartilage by partially suppressing the IL-1β-induced activation of both TLR3-TRIF-TBK1 and cGAS-STING-TBK1 signaling pathways in chondrocytes (Fig. 8). The balance of catabolism and anabolism in chondrocytes is critical for maintaining cartilage homeostasis. Among the anabolic proteins associated with cartilage, Collagen II and Aggrecan are the major ECM proteins [35].There is a consensus that catabolic enzymes, such as the MMPs (MMP1, MMP3, and MMP13) [36] and ADAMTS (ADAMTS4 and ADAMTS5) [37,38], play a key role in cartilage degradation. Proinflammatory factors, such as IL-1β, iNOS, and COX-2, stimulate the production of other cytokines, MMPs (MMP1, MMP3, and MMP13), ADAMTS4, ADAMTS5, and prostaglandins and decrease the synthesis of proteoglycans and Collagen II, leading to an imbalance in the homeostasis of anabolism and catabolism [39–42]. Previous studies have found that chondrocyte senescence affects cellular metabolic capacity and is thought to be involved in the development and progression of OA [5], as senescent chondrocytes have been found in human OA tissues [43]. Senescent cells can secrete senescence-associated secretory phenotype (SASP) factors, such as inflammatory cytokines and growth factors [44]. SASP factors secreted by senescent chondrocytes primarily include inflammatory factors and MMP degrading enzymes [45], which trigger excessive degradation of chondrocyte ECM. Cyclin-dependent kinase inhibitors are important signaling molecules that regulate cell proliferation. Representative molecules, such as $P16^{INK4a}$, $P21^{WAF1/CIP1}$, and P53, cause cell cycle arrest and promote cellular senescence [46]. SIRT1 reduces intracellular ROS levels by inhibiting the nuclear transcription factor NF-κB pathway, thereby delaying cellular senescence and regulating inflammation [47,48]. In this study, our *in vitro* results showed that in IL-1β-induced chondrocytes, the expression of inflammatory (iNOS and COX-2) and catabolic (MMP1, MMP3, MMP13, and ADAMTS5) indicators exhibited an upward trend, whereas that of anabolic markers (Collagen II and Aggrecan) was inhibited, which is consistent with the results of a previous study [49]. However, following treatment with BX795 in IL-1β-induced chondrocytes, the expression of these indicators was reversed. In addition, intra-articular injection of BX795 decreased the expression of MMP13, iNOS, and $P16^{INK4a}$, increased the expression of Collagen II and Aggrecan, and relieved the destruction of articular cartilage *in vivo*. These results suggest that when protecting articular cartilage from damage, BX795 exerts anti-inflammatory and anti-senescence effects, and improves the anabolism and catabolism of chondrocytes.TLRs are essential adaptor proteins for the TLR3/4-mediated innate immune response. Previous studies have shown that TLR3 is a ubiquitous receptor that mediates downstream signaling through TRIF [17,50]. TRIF-mediated signal transduction activates TBK1, contributes to the transcription of downstream genes such as IRF3, and activates the NF-κB signaling pathway, which results in an excessive inflammatory response and dysregulation of innate immunity [14,51,52]. STING is a transmembrane adaptor protein that is a key component of the innate immune response [53,54]. Upon stimulation by abnormal dsDNA in the cytoplasm, such as exogenous DNA contributed by pathogen infection and endogenous DNA leaked from the nucleus or mitochondria, second messenger cyclic-GMP–AMP (cGAMP) is produced in conjunction with cGAS. Then, cGAMP binds to STING and activates it. The activated cGAS–STING signaling pathway results in the recruitment and activation of TBK1, which activates IRF3 and NF-κB signaling, thus inducing an immune response, inflammatory response, cell senescence, and apoptosis [55–58]. The increased expression of cGAS may activate IRF3 and induce IFNβ in a STING-mediated manner [56]. In addition, a study has suggested that blocking the STING-dependent signaling pathway ameliorates the inflammatory response, senescence, and apoptosis and attenuates the development of degenerative diseases [16]. Indeed, our data showed that the expression of TRIF, cGAS, STING, and P-TBK1 was increased following IL-1β stimulation in chondrocytes. However, the administration of BX795 decreased the expression of these proteins in IL-1β-induced chondrocytes. These results suggest that the TBK1 inhibitor BX795 suppresses the activation of the TLR3–TRIF–TBK1 and cGAS–STING–TBK1 signaling pathways in IL-1β-induced chondrocytes.

To further clarify the specific mechanism of BX795 in protecting articular cartilage, the STING agonist DMXAA was used to selectively activate the STING signaling pathway, rather than the broad range of signaling pathways induced by IL-1β. The results indicated that the activation of the cGAS–STING signaling pathway upregulated the expression of catabolic proteins (MMP1, MMP3, and MMP13) and senescence-related proteins (P53, $P16^{INK4a}$, and $P21^{WAF1/CIP1}$) and downregulated the anabolic protein Aggrecan and the senescence-related protein (SIRT1). Conversely, BX795 reversed the expression of the above proteins in DMXAA-induced chondrocytes. Meanwhile, Poly (I:C), as an agonist of TLR3, which may trigger an inflammatory response by activating the TRIF–TBK1 signaling pathway instead of the many signaling pathways associated with IL-1β exposure [59], was used in our experiment. Similar to the proinflammatory effect of IL-1β, the expression levels of catabolic proteins (MMP1, MMP3, and MMP13) and senescence-related proteins (P53, $P16^{INK4a}$, and $P21^{WAF1/CIP1}$) were increase, whereas those of the anabolic protein Aggrecan and the senescence-related protein SIRT1 were decreased after the activation of the TRIF–TBK1 signaling pathway induced by Poly(I:C). However, the expression of the above proteins was reversed after the administration of BX795 in Poly(I:C)-induced chondrocytes, indicating that the degradation of the ECM and cell senescence in Poly(I:C)-induced chondrocytes may be alleviated by inhibiting the TRIF-mediated signaling pathway. Taken together, our findings indicate that the TBK1 inhibitor BX795 protects the articular cartilage by suppressing the activation of the cGAS–STING–TBK1 and TLR3–TRIF–TBK1 signaling pathways.

The MAPK and NF-κB signaling pathways play a crucial role in cell proliferation, differentiation, and inflammation regulation and are currently an active area of investigation because of their involvement in the pathology of OA chondrocytes [60]. The activation of MAPK and NF-κB signaling pathways increases the expression of iNOS, COX-2, MMPs, and ADAMTS5 and decreases the expression of Collagen II, Aggrecan, and SOX9, resulting in the degradation of the ECM and cartilage degeneration [61–63]. Therefore, inhibiting the activation of these two signaling pathways are considered treatment strategies for OA. Our results demonstrated that IL-1β induced the activation of MAPK and NF-κB signaling. However, the upregulated expression of P-JNK, P–P38, P-IKKα/β, P-IKBα, and P–P65 were downregulated by BX795, but it failed to change the expression of P-ERK in IL-1β-induced chondrocytes. Thus, our data suggest that BX795 protects articular cartilage by partially inhibiting IL-1β-induced activation of the MAPK and NF-κB signaling pathways in chondrocytes.

5. Conclusions

The TBK1 inhibitor BX795, which suppresses TBK1 phosphorylation, protects articular cartilage by partially inhibiting the MAPK and NF-KB signaling pathways via regulation of the cGAS–STING–TBK1 and

TLR3–TRIF–TBK1 signaling pathways. In addition, through inhibiting TLR3–TRIF–TBK1 and cGAS–STING–TBK1 signaling, BX795 ameliorates the inflammatory response, decreases cell senescence, and maintains the balance of anabolism and catabolism in chondrocytes. Furthermore, our findings demonstrate that TBK1 may be a potential therapeutic target in OA, thereby providing a theoretical basis for the treatment of OA.

6. Ethics statement

The study involving human and animal ethics was approved by the Ethics Committee of Tongji Hospital, Tongji Medical College, Huazhong University of Science and Technology (Ethics No: TJH-202107008, TJ-IRB20220478).

Author contributions

AC, SL, and RL were involved in the study concept and design; RL, YQ, ZW, and ZH performed the experiments; RL, SX, PC, and ZL collected the data and performed statistical analyses; RL prepared the manuscript; AC, SL, FG, HY, and JZ reviewed and revised the manuscript. All authors approved the publication.

Conflicts of interest

The authors declare no conflicts of interest.

Authorship & conflicts of interest STATEMENT

All persons who meet authorship criteria are listed as authors, and all authors certify that they have participated sufficiently in the work to take public responsibility for the content, including participation in the concept, design, analysis, writing, or revision of the manuscript. Each author certifies that this material or part thereof has not been published in another journal, that it is not currently submitted elsewhere, and that it will not be submitted elsewhere until a final decision regarding publication of the manuscript in Journal of Orthopaedic Translation has been made.

Indicate the specific contributions made by each author (list the authors' initials followed by their surnames, e.g., Y.L. Cheung). The name of each author must appear at least once in each of the three categories below.

Acknowledgments

This study was supported by the National Natural Science Foundation of China (No. 81672168) and Project Fund for Outstanding doctoral talents in Zhongnan Hospital of Wuhan University (ZNYB2023008).

Appendix A. Supplementary data

Supplementary data to this article can be found online at https://doi.org/10.1016/j.jot.2024.06.001.

References

[1] Hunter DJ, Bierma-Zeinstra S. Osteoarthritis. Lancet 2019;393(10182):1745–59.
[2] Dieppe PA, Lohmander LS. Pathogenesis and management of pain in osteoarthritis. Lancet 2005;365(9463):965–73.
[3] Hiligsmann M, Cooper C, Arden N, Boers M, Branco JC, Luisa Brandi M, et al. Health economics in the field of osteoarthritis: an expert's consensus paper from the European Society for Clinical and Economic Aspects of Osteoporosis and Osteoarthritis (ESCEO). Semin Arthritis Rheum 2013;43(3):303–13.
[4] Bolduc JA, Collins JA, Loeser RF. Reactive oxygen species, aging and articular cartilage homeostasis. Free Radic Biol Med 2019;132:73–82.
[5] Rim YA, Nam Y, Ju JH. The role of chondrocyte Hypertrophy and senescence in osteoarthritis initiation and progression. Int J Mol Sci 2020;21(7).
[6] Woodell-May JE, Sommerfeld SD. Role of inflammation and the immune system in the progression of osteoarthritis. J Orthop Res 2020;38(2):253–7.
[7] Hernández-Pedro N, Magana-Maldonado R, Ramiro AS, Pérez-De la Cruz V, Rangel-López E, Sotelo J, et al. PAMP-DAMPs interactions mediates development and progression of multiple sclerosis. Front Biosci (Schol Ed) 2016;8(1):13–28.
[8] Ahmed S, Maratha A, Butt AQ, Shevlin E, Miggin SM. TRIF-mediated TLR3 and TLR4 signaling is negatively regulated by ADAM15. J Immunol 2013;190(5):2217–28.
[9] Liu Y, Lu X, Qin N, Qiao Y, Xing S, Liu W, et al. STING, a promising target for small molecular immune modulator: a review. Eur J Med Chem 2021;211:113113.
[10] De Waele J, Verhezen T, van der Heijden S, Berneman ZN, Peeters M, Lardon F, et al. A systematic review on poly(I:C) and poly-ICLC in glioblastoma: adjuvants coordinating the unlocking of immunotherapy. J Exp Clin Cancer Res 2021;40(1):213.
[11] Shu C, Li X, Li P. The mechanism of double-stranded DNA sensing through the cGAS-STING pathway. Cytokine Growth Factor Rev 2014;25(6):641–8.
[12] Liu S, Guan W. STING signaling promotes apoptosis, Necrosis, and cell Death: an Overview and Update. Mediators Inflamm 2018;2018:1202797.
[13] Takeda K, Akira S. TLR signaling pathways. Semin Immunol 2004;16(1):3–9.
[14] Akira S, Takeda K, Kaisho T. Toll-like receptors: critical proteins linking innate and acquired immunity. Nat Immunol 2001;2(8):675–80.
[15] Matsumoto M, Seya T. TLR3: interferon induction by double-stranded RNA including poly(I:C). Adv Drug Deliv Rev 2008;60(7):805–12.
[16] Guo Q, Zhu D, Wang Y, Miao Z, Chen Z, Lin Z, et al. Targeting STING attenuates ROS induced intervertebral disc degeneration. Osteoarthritis Cartilage 2021;29(8):1213–24.
[17] Liang S, Wang ZG, Zhang ZZ, Chen K, Lv ZT, Wang YT, et al. Decreased RIPK1 expression in chondrocytes alleviates osteoarthritis via the TRIF/MyD88-RIPK1-TRAF2 negative feedback loop. Aging (Albany NY) 2019;11(19):8664–80.
[18] Zhou R, Zhang Q, Xu P. TBK1, a central kinase in innate immune sensing of nucleic acids and beyond. Acta Biochim Biophys Sin 2020;52(7):757–67.
[19] Geremia A, Biancheri P, Allan P, Corazza GR, Di Sabatino A. Innate and adaptive immunity in inflammatory bowel disease. Autoimmun Rev 2014;13(1):3–10.
[20] Ahmad L, Zhang SY, Casanova JL, Sancho-Shimizu V. Human TBK1: a Gatekeeper of neuroinflammation. Trends Mol Med 2016;22(6):511–27.
[21] Sun P, Xue Y. Silence of TANK-binding kinase 1 (TBK1) regulates extracellular matrix degradation of chondrocyte in osteoarthritis by janus kinase (JAK)-signal transducer of activators of transcription (STAT) signaling. Bioengineered 2022;13(1):1872–9.
[22] Hu SL, Mamun AA, Shaw J, Li SL, Shi YF, Jin XM, et al. TBK1-medicated DRP1 phosphorylation orchestrates mitochondrial dynamics and autophagy activation in osteoarthritis. Acta Pharmacol Sin 2022.
[23] Gao B, Yu W, Lv P, Liang X, Sun S, Zhang Y. Parkin overexpression alleviates cardiac aging through facilitating K63-polyubiquitination of TBK1 to facilitate mitophagy. Biochim Biophys Acta, Mol Basis Dis 2021;1867(1):165997.
[24] Scuderi SA, Lanza M, Casili G, Esposito F, Colarossi C, Giuffrida D, et al. TBK1 inhibitor exerts Antiproliferative effect on glioblastoma Multiforme cells. Oncol Res 2021;28(7):779–90.
[25] Jeon OH, Kim C, Laberge RM, Demaria M, Rathod S, Vasserot AP, et al. Local clearance of senescent cells attenuates the development of post-traumatic osteoarthritis and creates a pro-regenerative environment. Nat Med 2017;23(6):775–81.
[26] Glasson SS, Blanchet TJ, Morris EA. The surgical destabilization of the medial meniscus (DMM) model of osteoarthritis in the 129/SvEv mouse. Osteoarthritis Cartilage 2007;15(9):1061–9.
[27] Deuis JR, Dvorakova LS, Vetter I. Methods used to evaluate pain Behaviors in Rodents. Front Mol Neurosci 2017;10:284.
[28] Wei K, Shu Z, Pu H, Xu H, Li S, Xiao J, et al. Cystathionine-γ-lyase attenuates inflammatory response and pain of osteoarthritis. Int Immunopharmacol 2023;120:110289.
[29] Chinzei N, Rai MF, Hashimoto S, Schmidt EJ, Takebe K, Cheverud JM, et al. Evidence for Genetic contribution to Variation in Posttraumatic osteoarthritis in mice. Arthritis Rheumatol 2019;71(3):370–81.
[30] Glasson SS, Chambers MG, Van Den Berg WB, Little CB. The OARSI histopathology initiative - recommendations for histological assessments of osteoarthritis in the mouse. Osteoarthritis Cartilage 2010;18(Suppl 3):S17–23.
[31] Hwang HS, Lee MH, Choi MH, Kim HA. Induction of pro-inflammatory cytokines by 29-kDa FN-f via cGAS/STING pathway. BMB Rep 2019;52(5):336–41.
[32] Zhang Q, Hui W, Litherland GJ, Barter MJ, Davidson R, Darrah C, et al. Differential Toll-like receptor-dependent collagenase expression in chondrocytes. Ann Rheum Dis 2008;67(11):1633–41.
[33] You H, Zhang R, Wang L, Pan Q, Mao Z, Huang X. Chondro-protective effects of Shikimic acid on osteoarthritis via Restoring Impaired autophagy and suppressing the MAPK/NF-κB signaling pathway. Front Pharmacol 2021;12:634822.
[34] Herrero-Beaumont G, Pérez-Baos S, Sánchez-Pernaute O, Roman-Blas JA, Lamuedra A, Largo R. Targeting chronic innate inflammatory pathways, the main road to prevention of osteoarthritis progression. Biochem Pharmacol 2019;165:24–32.
[35] Luo Y, Sinkeviciute D, He Y, Karsdal M, Henrotin Y, Mobasheri A, et al. The minor collagens in articular cartilage. Protein Cell 2017;8(8):560–72.
[36] Dahlberg L, Billinghurst RC, Manner P, Nelson F, Webb G, Ionescu M, et al. Selective enhancement of collagenase-mediated cleavage of resident type II collagen in cultured osteoarthritic cartilage and arrest with a synthetic inhibitor that spares collagenase 1 (matrix metalloproteinase 1). Arthritis Rheum 2000;43(3):673–82.
[37] Fosang AJ, Little CB. Drug insight: aggrecanases as therapeutic targets for osteoarthritis. Nat Clin Pract Rheumatol 2008;4(8):420–7.

[38] Larkin J, Lohr TA, Elefante L, Shearin J, Matico R, Su JL, et al. Translational development of an ADAMTS-5 antibody for osteoarthritis disease modification. Osteoarthritis Cartilage 2015;23(8):1254–66.
[39] Wang T, He C. Pro-inflammatory cytokines: the link between obesity and osteoarthritis. Cytokine Growth Factor Rev 2018;44:38–50.
[40] McAllister MJ, Chemaly M, Eakin AJ, Gibson DS, McGilligan VE. NLRP3 as a potentially novel biomarker for the management of osteoarthritis. Osteoarthritis Cartilage 2018;26(5):612–9.
[41] Sellam J, Berenbaum F. The role of synovitis in pathophysiology and clinical symptoms of osteoarthritis. Nat Rev Rheumatol 2010;6(11):625–35.
[42] Lepetsos P, Papavassiliou KA, Papavassiliou AG. Redox and NF-κB signaling in osteoarthritis. Free Radic Biol Med 2019;132:90–100.
[43] Price JS, Waters JG, Darrah C, Pennington C, Edwards DR, Donell ST, et al. The role of chondrocyte senescence in osteoarthritis. Aging Cell 2002;1(1):57–65.
[44] Campisi J. Senescent cells, tumor suppression, and organismal aging: good citizens, bad neighbors. Cell 2005;120(4):513–22.
[45] Philipot D, Guérit D, Platano D, Chuchana P, Olivotto E, Espinoza F, et al. p16INK4a and its regulator miR-24 link senescence and chondrocyte terminal differentiation-associated matrix remodeling in osteoarthritis. Arthritis Res Ther 2014;16(1):R58.
[46] Hernandez-Segura A, Nehme J, Demaria M. Hallmarks of cellular senescence. Trends Cell Biol 2018;28(6):436–53.
[47] Shen P, Deng X, Chen Z, Ba X, Qin K, Huang Y, et al. SIRT1: a potential therapeutic target in autoimmune diseases. Front Immunol 2021;12:779177.
[48] Yang Y, Liu Y, Wang Y, Chao Y, Zhang J, Jia Y, et al. Regulation of SIRT1 and its roles in inflammation. Front Immunol 2022;13:831168.
[49] Lu R, He Z, Zhang W, Wang Y, Cheng P, Lv Z, et al. Oroxin B alleviates osteoarthritis through anti-inflammation and inhibition of PI3K/AKT/mTOR signaling pathway and enhancement of autophagy. Front Endocrinol 2022;13:1060721.
[50] Yamamoto M, Sato S, Hemmi H, Hoshino K, Kaisho T, Sanjo H, et al. Role of adaptor TRIF in the MyD88-independent toll-like receptor signaling pathway. Science 2003;301(5633):640–3.
[51] Honda K, Taniguchi T. IRFs: master regulators of signalling by Toll-like receptors and cytosolic pattern-recognition receptors. Nat Rev Immunol 2006;6(9):644–58.
[52] Liu S, Cai X, Wu J, Cong Q, Chen X, Li T, et al. Phosphorylation of innate immune adaptor proteins MAVS, STING, and TRIF induces IRF3 activation. Science 2015;347(6227):aaa2630.
[53] Ishikawa H, Barber GN. STING is an endoplasmic reticulum adaptor that facilitates innate immune signalling. Nature 2008;455(7213):674–8.
[54] Zhong B, Yang Y, Li S, Wang YY, Li Y, Diao F, et al. The adaptor protein MITA links virus-sensing receptors to IRF3 transcription factor activation. Immunity 2008;29(4):538–50.
[55] Sun L, Wu J, Du F, Chen X, Chen ZJ. Cyclic GMP-AMP synthase is a cytosolic DNA sensor that activates the type I interferon pathway. Science 2013;339(6121):786–91.
[56] Wu J, Sun L, Chen X, Du F, Shi H, Chen C, et al. Cyclic GMP-AMP is an endogenous second messenger in innate immune signaling by cytosolic DNA. Science 2013;339(6121):826–30.
[57] Ishikawa H, Ma Z, Barber GN. STING regulates intracellular DNA-mediated, type I interferon-dependent innate immunity. Nature 2009;461(7265):788–92.
[58] Guo Q, Chen X, Chen J, Zheng G, Xie C, Wu H, et al. STING promotes senescence, apoptosis, and extracellular matrix degradation in osteoarthritis via the NF-κB signaling pathway. Cell Death Dis 2021;12(1):13.
[59] Wang Y, Wang K, Fu J. HDAC6 mediates poly (I:C)-Induced TBK1 and Akt phosphorylation in Macrophages. Front Immunol 2020;11:1776.
[60] Moon SM, Lee SA, Han SH, Park BR, Choi MS, Kim JS, et al. Aqueous extract of Codium fragile alleviates osteoarthritis through the MAPK/NF-κB pathways in IL-1β-induced rat primary chondrocytes and a rat osteoarthritis model. Biomed Pharmacother 2018;97:264–70.
[61] Marcu KB, Otero M, Olivotto E, Borzi RM, Goldring MB. NF-kappaB signaling: multiple angles to target OA. Curr Drug Targets 2010;11(5):599–613.
[62] Sondergaard BC, Schultz N, Madsen SH, Bay-Jensen AC, Kassem M, Karsdal MA. MAPKs are essential upstream signaling pathways in proteolytic cartilage degradation–divergence in pathways leading to aggrecanase and MMP-mediated articular cartilage degradation. Osteoarthritis Cartilage 2010;18(3):279–88.
[63] Ushita M, Saito T, Ikeda T, Yano F, Higashikawa A, Ogata N, et al. Transcriptional induction of SOX9 by NF-kappaB family member RelA in chondrogenic cells. Osteoarthritis Cartilage 2009;17(8):1065–75.